

Recent Progress in Bionic Skin Based on Conductive Polymer Gels

Huijing Li, Guorong Gao,* Zhenyu Xu, Diane Tang, and Tao Chen*

Bionic skin sensors based on conductive polymer gels have garnered interest for their potential applications in human-computer interaction, soft robotics, biomedical systems, sports, and healthcare, because of their intrinsic flexibility and stretchability embedded at the material level, and other such as self-healing, adhesion, high, and low temperature tolerance properties that can be tuned through macromolecular design. Here, important advances in polymer gel-based flexible sensors over recent years are summarized, from material design, sensor fabrication to system-level applications. This review focuses on the representative strategies of design and preparing of conductive polymer gels, and adjusting their conductivity, mechanics, and other properties such as self-healing and adhesiveness by controlling the macromolecular network structures. The state-of-art of present flexible pressure and strain sensors, temperature sensors, position sensors, and multifunctional sensors based on capacitance, voltage, and resistance sensing technologies, are also systematically reviewed. Finally, perspectives on issues regarding further advances and challenges are provided.

Skin as the largest organ that encompasses the entire body can be used to sense touch, temperature, pain, itch, etc.^[1–4] There are various types of sensory receptors in human skin, including nociceptors, which sense painful stimuli; pruriceptors, which sense itch; thermoreceptors, which convey temperature information; four kinds of mechanoreceptors,^[5] that is, two types of slow adapting receptors, which respectively respond to sustained pressure and skin stretch, and two types of fast adapting receptors, which respectively measure low-frequency (5–50 Hz) and high-frequency vibrations (up to 400 Hz). Sensing signals from receptors are transported through nerve fibers, then interpreted by brain to give complex information about limb bending and object hardness, shape,^[2] etc. Learning from human skins, designing sensing materials that mimic skin mechanics and

1. Introduction

Flexible and stretchable sensors are the key basic components of future flexible electronics and have broad application prospects in the fields of Internet of Things, human-computer interaction, humanoid soft robots, intelligent medical apparatus, and instruments. The compliance and deformability of flexible sensors enabled them to adapt to human or soft robot bodies like skin, and to perform tasks that cannot be accomplished by rigid sensors.

sensing performance in full aspects, and ultimately constructing bionic intelligent sensing systems are increasingly seen as a worthwhile endeavor.^[6–9]


Polymer gels, including hydrogels, organic gels,^[10,11] and ionic liquid gels^[12] are physically or chemically cross-linked three-dimensional polymer networks that contain mobile liquids.^[13] They have network structures resembling that of extracellular matrix. Most polymer gels have similar moduli with muscle and skin tissues.^[14,15] Some of them are biocompatible, transparent,^[16,17] self-healing upon mechanical damage,^[18–21] adhesive to various substrates,^[22,23] anti-freezing, resistant to high temperature, and able to work in extreme climate environment.^[23–26] Polymer gels can conduct electricity based on ionic^[23,24,27–29] or electronic conduction mechanisms.^[29–36] Moreover, they are flexible to adjust the all those properties by changing the constituents of the precursor.^[23,27,28,31,37] With the development of flexible and wearable electronic devices, conductive polymer gels have been widely studied as energy collection and storage devices,^[38,39] diodes,^[40,41] displays,^[42] and actuators.^[28] They have also been developed based on mechanisms of capacitance,^[16,43] voltage,^[44] and resistance^[45] changes upon change of physical conditions, and are able to sense pressure,^[43,45] strain,^[46–49] finger approaching, and leaving,^[50] touch position,^[16] ambient temperature,^[45] and humidity.^[51,52] Thus, they have natural advantages as bionic skin sensors.

This review aims to provide a summary of the general ways for preparing conductive polymer gels and then constructing bionic

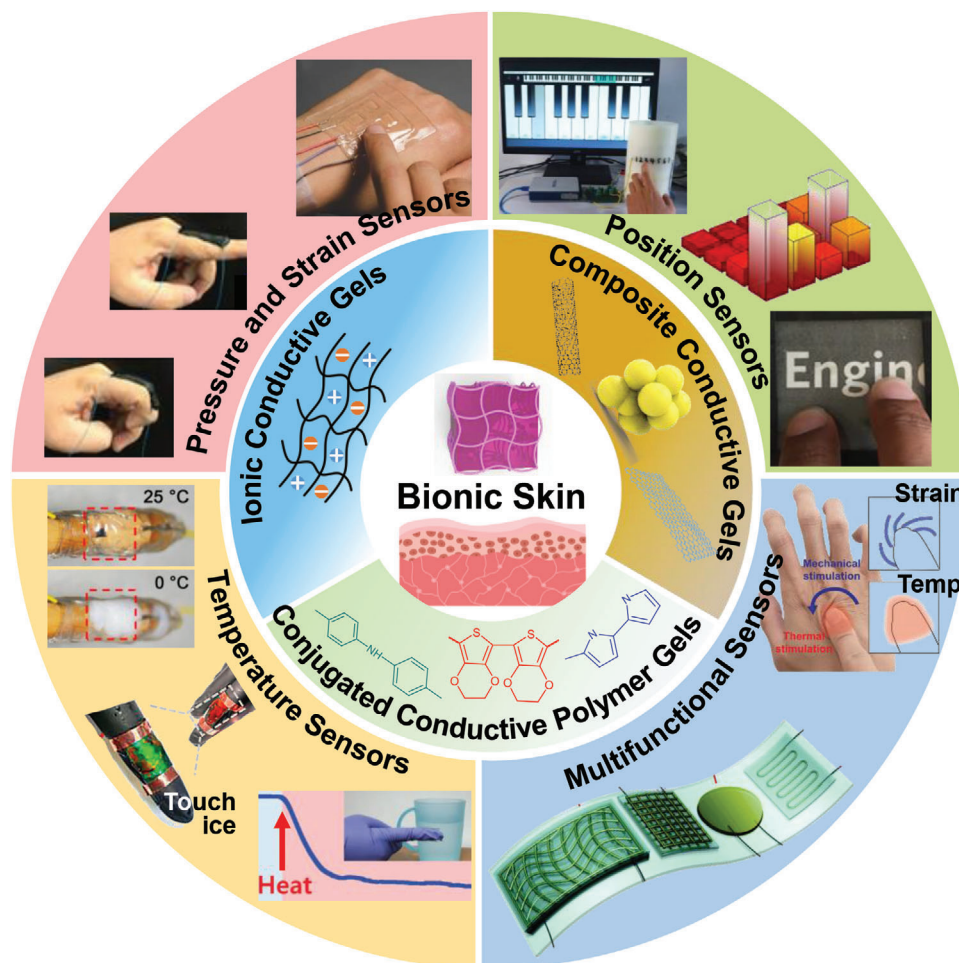
H. Li, G. Gao, Z. Xu, T. Chen
 Key Laboratory of Marine Materials and Related Technologies
 Zhejiang Key Laboratory of Marine Materials and Protective Technologies
 Ningbo Institute of Materials Technology and Engineering,
 Chinese Academy of Sciences
 Ningbo 315201, China
 E-mail: gaogr@nimte.ac.cn; tao.chen@nimte.ac.cn

H. Li, G. Gao, Z. Xu, T. Chen
 School of Chemical Science
 University of Chinese Academy of Sciences
 9A Yuquan Road, Beijing 100049, China

D. Tang
 YK Pao School
 No 1800, Lane 900 North Sanxin Road, Songjiang District,
 Shanghai 201620, China

 The ORCID identification number(s) for the author(s) of this article can be found under <https://doi.org/10.1002/marc.202100480>

DOI: 10.1002/marc.202100480



Scheme 1. Overview of the construction strategies and promising applications of conductive polymer gels as bionic skin sensors, including pressure and strain sensors, temperature sensors, position sensors and multifunctional sensors. Pressure and strain sensors: Reproduced with permission.^[55] 2018, American Association for the Advancement of Science (AAAS) (bottom left); Reproduced with permission.^[43] 2014, Wiley-VCH GmbH (top left); Position sensors: Reproduced with permission.^[92] 2020, Wiley-VCH GmbH (top right); Reproduced with permission.^[17] 2017, AAAS (bottom right); Multifunctional sensors: Reproduced with permission.^[100] 2020, AAAS (top right); Reproduced with permission.^[101] 2019, The Royal Society of Chemistry (bottom right); Temperature sensors: Reproduced with permission.^[45] 2021, American Chemical Society (top left); Reproduced with permission.^[91] 2020, National Academy of Sciences (central left); Reproduced with permission.^[90] 2019, Wiley-VCH GmbH (bottom left).

skin sensors. It is presented as following (Scheme 1). First, the molecular structures, properties and preparation of three types of gels used in bionic skin sensors in recent years, that is, ionic conductive gels, composite conductive gels, and conjugated conductive polymer gels, are introduced in detail. The advantages and disadvantages of their respective performance and the corresponding suitable application situations are systematically analyzed. Then, we presented the preparation methods of pressure and strain sensors, temperature sensors, and position sensors based on capacitance, voltage, and resistance sensing technologies, as well as the representative building strategies for multifunctional and multimodal sensor systems. Subsequently, the merits and limitations of the sensors based on different sensing technologies were compared. Finally, we discussed the opportunities and challenges faced, while outlining major open questions in the area of bionic skin sensors based on polymer gels. We hope this review will motivate new research effort and encourage further interest in this field.

2. Conductive Polymer Gels

2.1. Ionic Conductive Gels

Ionic conductive gels are polymer gels that have absorbed mobile ions, including hydrogels, ionic liquid gels, and organogels,^[11] etc. Electrical current is conducted by the migration of ions that results from adding inorganic salt, or ionic liquid and the conductivity could be simply tuned by the quantity of ions. Ionic conductive gels are usually endowed with stretchability,^[12,42,53] compliance,^[54,55] adhesive,^[39,55] self-healing ability,^[39,54,55] shape memory,^[56] and transparent properties^[24,39] by changing the precursor content and designing the polymer structure. They are promising materials for bionic skin,^[26,57–61] which are flexible ionic conductive polymer sensors that mimic the sensing functions of mammalian skin.

For accurate sensing, an artificial skin sensor needs to be mechanically compliant and durable. Lei et al. reported a

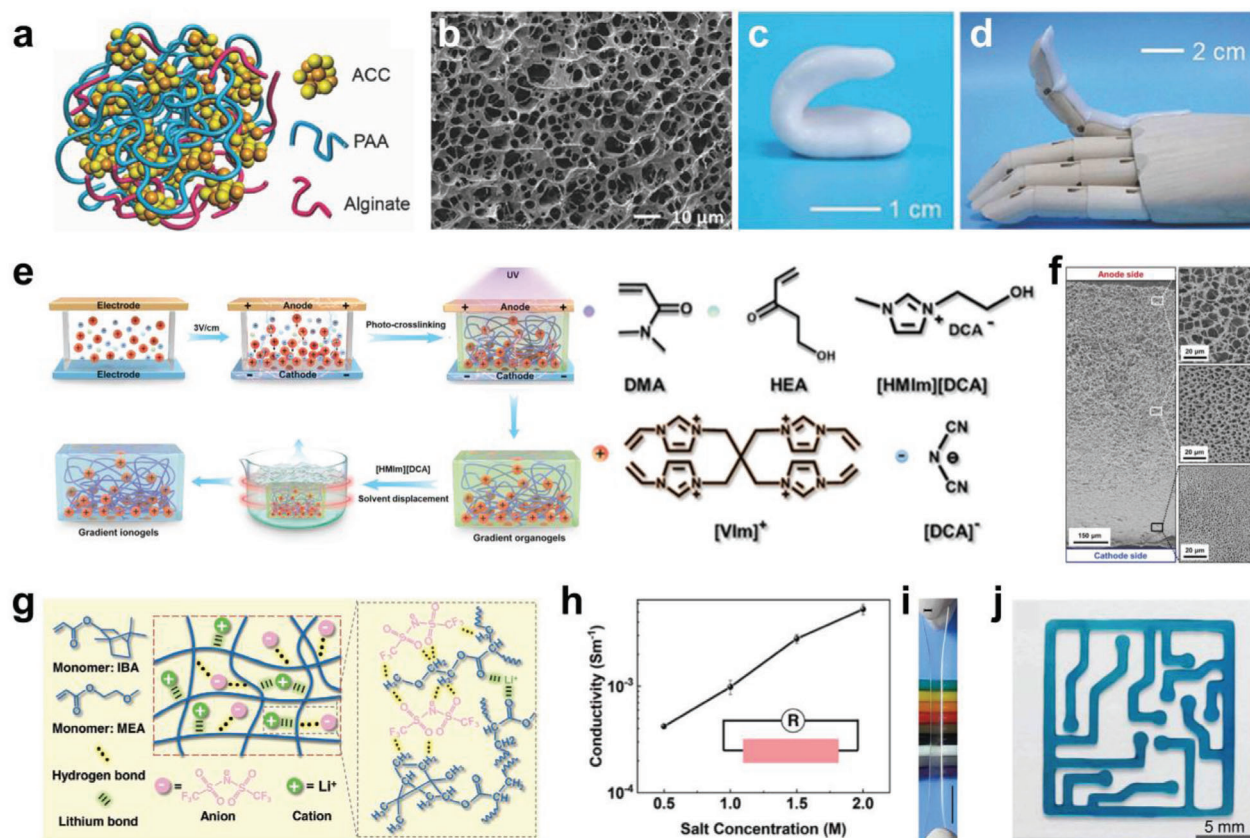


Figure 1. a) Schematic structure of the ACC/PAA/alginate mineral hydrogel. b) SEM image of a freeze-dried hydrogel. Photos show the hydrogels are c) mouldable and d) compliant. Reproduced with permission.^[54] Copyright 2017, Wiley-VCH GmbH. e) Schematic illustration of fabrication and monomers, cross-linkers, and ionic liquids for synthesis of the gradient ionic liquid gel. f) SEM image of a freeze-dried gradient gel. Reproduced with permission.^[62] Copyright 2021, Wiley-VCH GmbH. (g) Schematic illustration of molecular design of the liquid-free ionic conductive elastomer (ICE). h) Conductivity of ICEs varied by lithium salt concentrations. i) A photo of a transparent and stretchable ICE. j) A flexible printing circuit made by 3D printing with ICEs as ink. Reproduced with permission.^[63] Copyright 2021, Wiley-VCH GmbH.

hydrogel composed of polyacrylic acid (PAA) and alginate physically cross-linked by amorphous calcium carbonate nanoparticles (ACC) (Figure 1a),^[54] which has interconnected porous architecture (Figure 1b). The physically cross-linked macromolecules endowed hydrogel with large ultimate tensile strain, self-healing ability, mouldability, (Figure 1c) and compliance (Figure 1d). Ca²⁺ from ACC serve as ion carriers to make it conductivity. The hydrogel was demonstrated as the conductive layer in capacitance sensor to sense pressure.

It remains a challenge to simultaneously realize high sensitivity and broad detection range on flexible sensors. Ren et al. reported an ionic liquid gel with gradient microstructure, resulted from the gradient density of the cationic cross-linker (tetravinylimidazolium, [VIm]⁺, Figure 1e) in electric field.^[62] The Young's moduli at low and high density sides are <10 kPa and >10 MPa, respectively (Figure 1f). For capacitive sensors with the ionic liquid gels acting as electrodes, the sensitivity was as high as 1.62 nF kPa⁻¹ in low Young's modulus region, and the detection range was 3 × 10² to 2.5 × 10⁶ Pa. Ionic liquids also endow the gels with long-term low- and high- temperature tolerance (200 °C / -80 °C).

The leakage and evaporation of liquids affect the properties and service time of polymer gels. Jia et al. developed a liquid-

free ionic conductive elastomers (ICEs) that composed of copolymer networks of ethylene glycol methyl ether acrylate (MEA) and isobornyl acrylate (IBA). Additionally, this ICE contains the salt lithium bis(trifluoromethane) sulfonamide (LiTFSI) (Figure 1g),^[63] which makes the ICEs conductive, with the conductivity increases from 4.20 × 10⁻⁴ to 5.28 × 10⁻³ S m⁻¹ as the salt content increases from 0.5 to 2.0 M (Figure 1h). The ICE is transparent and highly stretchable (Figure 1i), and is demonstrated to be used as 3D printing inks to prepare flexible printing circuit (Figure 1j).

Compared with metal, carbon materials, composite conductive gels, and conjugate conductive polymer hydrogels, ionic conductive gels have unique advantages. First, the charge carriers of ionic conductive gel are free ions, while other materials conduct electricity by using electrons. The macromolecular network structure and ionic conductivity of ionic conductive gel are similar to natural tissue, so it has natural advantages in studying, verifying bio-sensing mechanisms, and making bionic sensors. Second, the mobile ions dissolve in liquid phase of the gel, so its ionic conductivity is affected by deformation negligibly. The resistance change of ionic conductive gel during stretching could be predicted by $R/R_0 = \lambda^2$, where R is the resistance, R_0 is the initial resistance, λ denotes that the gel is stretched to λ

times.^[13] However, other conductors, such as silver nanowires or carbon nanotube composites, exhibit sharp and unpredictable changes in conductivity when stretched. Obviously, ionic conductive gels are more suitable for making stretchable electronic devices. Third and most importantly, ionic conductive gels are highly transparent to visible light compared with other stretchable conductive materials, such as composite conductive gels and conjugated polymer conductive gels are difficult to achieve high transparency due to the necessary aggregation and interconnection of nanoscale particles or strips. This combination of those advantages make ionic conductive gels become ideal materials for flexible electronic devices such as artificial skins,^[64] artificial muscles,^[65] touch panels,^[16] and luminescent devices.^[42]

On the other hand, there are also several disadvantages for ionic conductive gels. Electrochemical reactions occur at the interface between gel and metal electrode, which cause the current in gel to continue changing over time. Ionic conductivity is prone to be affected by temperature and humidity significantly. These problems cannot be avoided if ionic conductive gels are developed as commercial products.

2.2. Composite Conductive Gels

Composite conductive gels are gels composited with conductive fillers, such as micrometer or nanometer sized metal,^[22,31,66] carbon particles,^[29,30] and MXene.^[23,67] There are several advantages for composite conductive gels using as bionic electronics. First, the conductivity can be accurately adjusted in a wide range by changing amounts of fillers. Second, the mechanical properties are tunable through tailoring the intermolecular interactions between polymers and fillers. Third, benefiting from researches about multilevel structure nanocomposite polymer materials, it is feasible to design and fabricate diverse composite conductive gels and devices with various structures, properties and bionic sensing functions. The disadvantage is the strategy of constructing percolation conductive network, which based on the aggregation of nano- or micro-fillers, leads to opaque inevitably, thus, it restricts the application of this kind of materials.

Most conductive gels have low electrical conductivity ($< 100 \text{ S cm}^{-1}$), and are inadequate for digital circuits and bioelectronics. Ohm et al. reported a hydrogel composite with high conductivity (374 S cm^{-1}), soft compliance (Young's modulus $< 10 \text{ kPa}$) and high stretchability (250% strain).^[66] Micrometer-sized silver flakes were first mixed in the polyacrylamide-alginate hydrogel precursor solution. For achieving high conductivity, the hydrogel was subjected to partial dehydration (Figure 2a). From SEM images, adjacent silver flakes were separated by polymer matrix before dehydration (Figure 2b, left), while forming a percolating network after dehydration (Figure 2b, right). Concomitantly, conductivity increased from 0.13 to 374 S cm^{-1} after dehydration of the hydrogel (Figure 2b). The composite hydrogels showed potential usage as neuromuscular electrical stimulation electrode.

Cai et al. presented a heterostructured conductive nanomaterial that couples vinyl-hybrid-silica nanoparticle (VSNP)-modified polyacrylamide hydrogel with MXene layer through the bridging of polypyrrole nanowires (PpyNWs) at the interfaces (Figure 2c).^[67] MXene and PpyNWs were coated on the

hydrogel surface through a layer by layer process. The heterogeneous material acts as a resistance sensor upon stretch, with the gauge factor scale linearly until 800% strain. Capacitive sensor was also fabricated by assembling two pieces of heterostructured hydrogels with MXene sides placed back to back. Its capacitance changed by the pressure and a finger approaching, and also showed a subtle dependence on temperature and light.

Recently, we reported an asymmetric carbon nanotubes (CNTs)-elastomer/poly(*N*-isopropylacrylamide) (PNIPAm) bilayer by coating CNTs on Ecoflex elastomer, then synthesizing PNIPAm hydrogel on another side of Ecoflex (Figure 2d).^[68] The hydrogel was covalently cross-linked onto Ecoflex by using benzophenone as cross-linker (Figure 2e). The deformation of hydrogel was monitored through resistance change of CNTs layer (Figure 2f).

2.3. Conjugated Conductive Polymer Gels

Conjugated conductive polymers are a series of polymers with electrons held in their backbones. Delocalized π -electrons act as charge carriers moving freely along the unsaturated backbone. Poly(3,4-ethylenedioxythiophene) polystyrene sulfonate (PEDOT:PSS),^[31,33,34] polyaniline (PANi),^[69,70] and polypyrrole (Ppy)^[35] are typical conjugated conductive polymers, with conductivities comparable to those of semiconductors and metals. Conventional conjugated conductive polymers with modulus in order of 1 GPa are not much stretchy, thus, mechanically mismatch skin. There is a strong demand for soft and stretchable conjugated conductive polymer materials with excellent electrical conductivity.^[71,72] Combining polymer gels with conjugated conducting polymers is a promising approach.

PEDOT:PSS is a biocompatible conjugated polymer.^[73–75] PEDOT:PSS hydrogels, prepared by blending with hydrogel precursors, suffer from low conductivity ($0.2\text{--}2.2 \text{ S m}^{-1}$). The low performance may arise from the disconnected aggregates of conjugated polymer.^[76] Feig et al. reported an interpenetrating network PEDOT:PSS hydrogel.^[33] In which, a single network PEDOT:PSS hydrogel was first formed by increasing the ionic strength of PEDOT:PSS aqueous dispersions, as the electrostatic repulsion between PEDOT:PSS particles were screened, which resulted in physical cross-linking of π - π stacking.^[77] Then, the PEDOT:PSS gel was infiltrated with acrylic acid monomers before polymerization (Figure 3a). The interpenetrating network hydrogels could be stretched to over 250% (Figure 3b), and their modulus ($8\text{--}374 \text{ kPa}$) was tunable by changing the contents and the crosslinking density of polyacrylic acid. The hydrogels have high conductivity ($>10 \text{ S m}^{-1}$), due to the well connected PEDOT:PSS networks.

Lu et al. proposed that mixing or in situ polymerization of conjugated polymers within non-conductive polymers leads to potentially compromise conductivity of the resulted materials, as the non-conductive polymer acts as an insulator.^[31,78] They demonstrated a pure PEDOT:PSS hydrogel with extraordinary electrical, mechanical, and swelling properties.^[31] The hydrogel was prepared by dry-annealing of PEDOT:PSS aqueous solution, and then reswelling in water (Figure 3c). After dry-annealing, PEDOT:PSS undergoes phase separation into three different domains, that is, PEDOT-rich crystalline region,

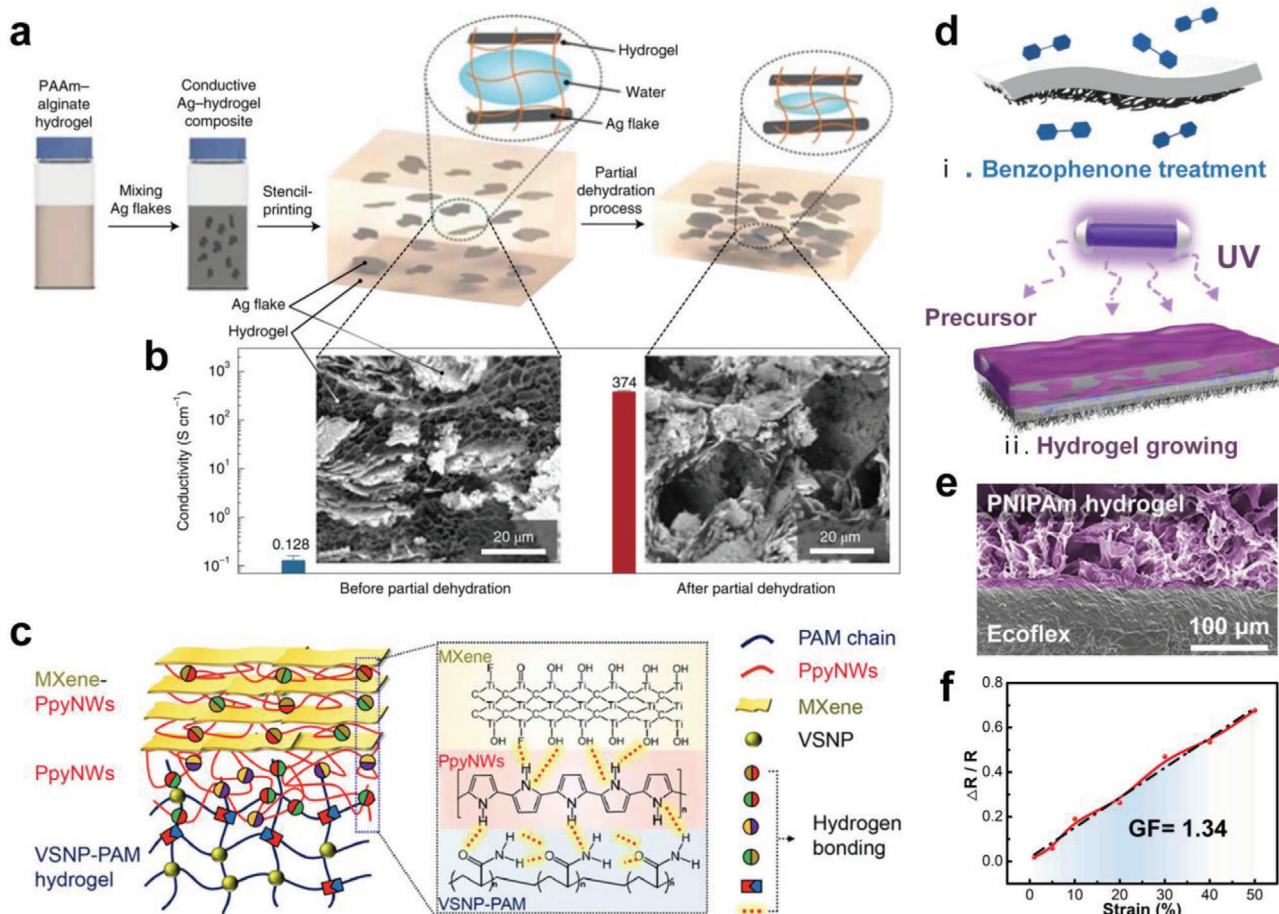


Figure 2. a) Schematic illustration of fabrication of silver flakes composites hydrogels. b) Conductivity and micrographs of the composite before and after dehydration. Reproduced with permission.^[66] Copyright 2021, Nature Publishing Group. c) Schematic illustration of the MXene-PpyNW-VSNP-polyacrylamide (PAM) layer-by-layer structure. Reproduced with permission.^[67] Copyright 2020, American Association for the Advancement of Science (AAAS). e) Schematic illustration of fabrication of asymmetric CNTs-elastomer/PNIPAm bilayer.^[68] f) SEM image and g) plot of resistance changed by tensile strain of the bilayer. Reproduced with permission.^[68] Copyright 2021, Elsevier.

PEDOT:PSS semi-crystalline region, and PSS-rich soft region. After reswelling, the hydrophilic PSS-rich region fully swells, while PEDOT:PSS nanofibrils maintain the interconnected networks, which results in a stable hydrogel (Figure 3c). The hydrogels exhibit high conductivity ($\approx 20 \text{ S cm}^{-1}$ in PBS), high stretchability ($> 35\%$) and low Young's modulus ($\approx 2 \text{ MPa}$). A hydrogel wavy mesh is fabricated by printing PEDOT:PSS aqueous dispersion, dry-annealing and then rehydrating (Figure 3d).

Pan et al. reported an ultra-sensitive pressure sensor based on polypyrrole hydrogels with hollow-sphere microstructure.^[35] The hollow-sphere morphology was achieved by a multiphase reaction mechanism (Figure 3e): an aqueous solution of oxidative reagent was mixed with pyrrole monomer, isopropanol and phytic acid (dopant) until an emulsion is formed, followed by rapid gelation. The resultant hydrogel was purified in water, and dehydrated to form film. The hollow-sphere structure enabled the polypyrrole to elastically deform under pressure (Figure 3f). High sensitive resistive pressure sensor was obtained after micropatterning the film surface, with sensitivity of $\approx 56.0\text{--}133.1 \text{ kPa}^{-1}$ in low-pressure regime ($< 30 \text{ Pa}$), which surpasses the subtle pressure sensing properties of the natural skin.

3. Bionic Skin Sensors

3.1. Pressure and Strain Sensors

Polymer gel pressure and strain sensors are the most widely studied, because they have the most promising applications, including wearing exercising/health state monitoring,^[54,66,67] robotics movement analysis,^[68] and so on. The pressure sensors are expected to have low detection limits, while the strain sensors require large sensitivity in a wide deformation range. The sensors monitor pressure and strain by detecting the electrical parameters, such as resistance, capacitance, and voltage. Due to the diversity of polymer gels, these sensors are ultra-stretchable, self-healing, adhesive, and able to service in aquatic environments,^[79] or able to all-roundly mimic the properties and sensation of skin.^[80–84]

Zhang et al. demonstrated that hydrogel composites incorporating MXene outperform all reported hydrogels for strain sensors.^[55] This hydrogel was prepared by mixing MXene nanosheets with a commercial poly(vinyl alcohol) (PVA) hydrogel, namely “crystal clay”. The composite hydrogel exhibits

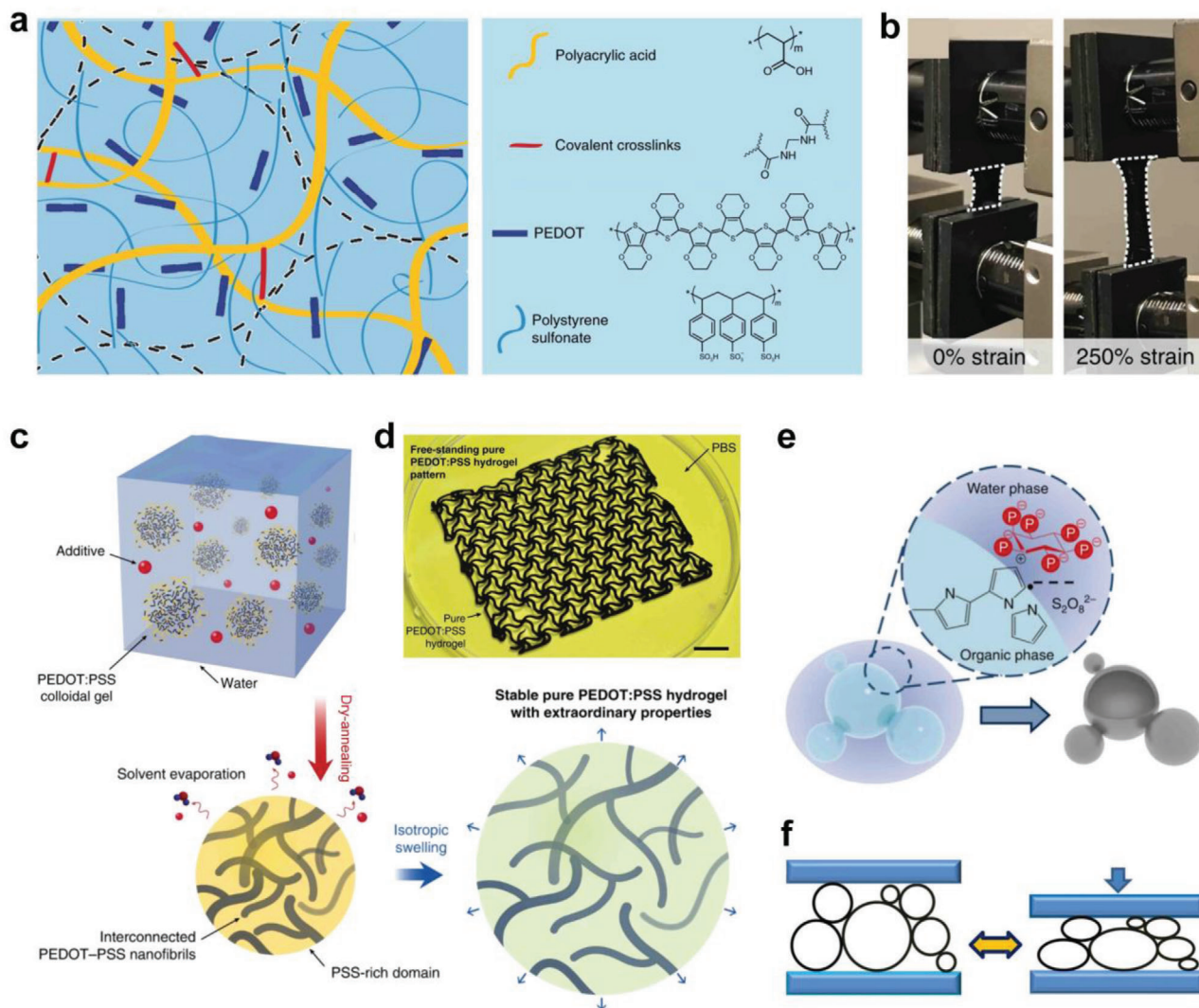


Figure 3. a) Schemes show structure of the interpenetrating networks PEDOT:PSS hydrogel. b) Picture of a corresponding hydrogel being stretched to strain of 250%. Reproduced with permission.^[33] Copyright 2018, Nature Publishing Group. c) Schematic illustration of the preparing process of pure PEDOT:PSS hydrogel. d) Photo of a pure PEDOT:PSS hydrogel with wave mash pattern. Scale bar, 8 mm. Reproduced with permission.^[31] Copyright 2019, Nature Publishing Group. Schematics of e) the interphase synthesis mechanism of Ppy hydrogels with hollow-sphere microstructures, and f) the structural elasticity of the hollow-sphere-structured Ppy. Reproduced with permission.^[35] Copyright 2014, Nature Publishing Group.

impressive stretchability of more than 3400% (Figure 4a). Its resistance increases upon tensile deformation, wherein the distance between MXene sheets increases, and their chance of contacting in hydrogel matrix reduces (Figures 4b and 5c). In contrast, its resistance decreases under compressive deformation, wherein the separation between MXene becomes less and their chance of contacting increases (Figures 4b and 5c). It exhibits outstanding tensile strain sensitivity with a gauge factor (GF) of 25, and much higher compressive strain sensitivity with a GF of 80. Because of the conformable, sticky, and stretchable characteristics, the hydrogel can adhere to various positions on human body to detect various bodily motions. The sensing signals were clear, stable and not delayed (Figure 4d).

Ge et al. reported an ionic conductive binary networked polyacrylamide/polyvinyl alcohol hydrogel resistance sensor.^[46] The hydrogel has impressive stretchability (> 500%) and high sen-

sitivity (0.05 kPa^{-1}). The sensor can detect tiny physiological activities such as phonation, airflowing and saliva swallowing, and extensive body motions such as finger and arm bending. They further developed a fiber-reinforced self-healing hydrogel strain sensor.^[85] To fully mimic the microstructures of human muscle, which consists of epimysium, fascicle components and muscle fiber with muscular tissue, they introduced polyaniline nanofibers into the poly(acrylic acid) hydrogel. Reversible physical association generated multiscale nanoarchitectures within hydrogel, including metal ions (Fe^{3+})-coordination, hydrogen bonding, and electrostatic interactions, which further account for impressive stretchability (991%) and high healing efficiency (90.8%). The hydrogel resistance sensor has high gauge factor (18.8) within broad strain range (268.9%), and can differentiate signature writing, exhibiting promising potential usage as wearable touch keyboard.

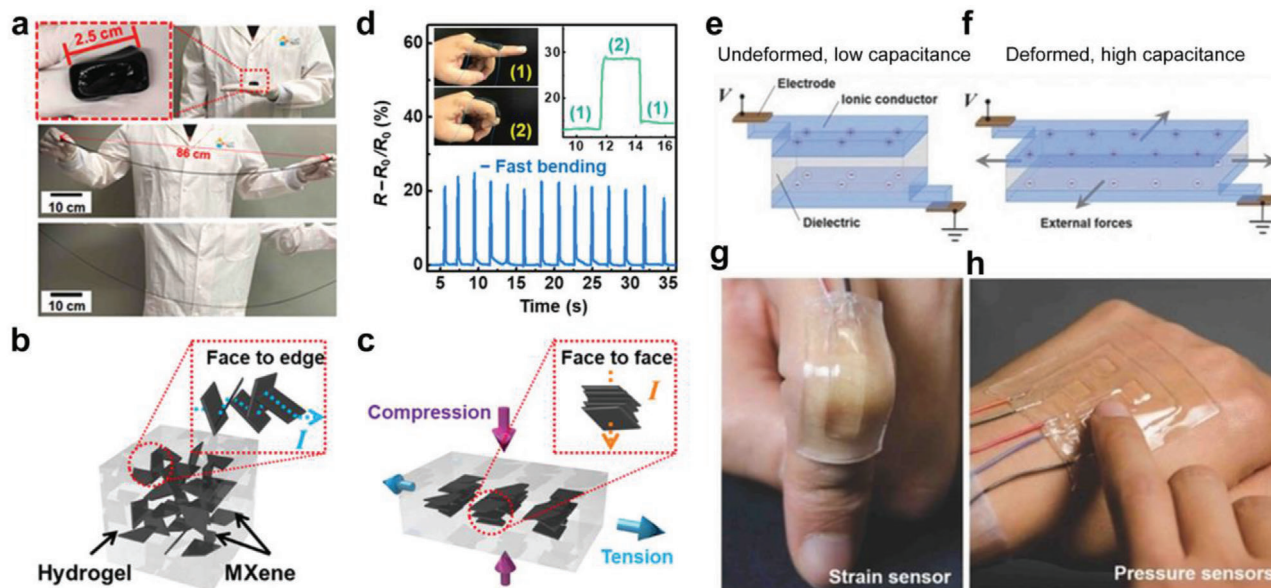


Figure 4. a) Photographs demonstrating the stretchability of MXene hydrogel. b,c) Schematics illustration of mechanism of electromechanical responses of MXene hydrogel.^[55] d) Resistance change of MXene hydrogel sensor in response to finger bending. Reproduced with permission.^[55] Copyright 2018, AAAS. Schematics illustration of the architectures of hydrogel capacitance sensor e) in absence of and f) under external forces.^[43] Photos show g) a capacitance sensor attached on finger to detect finger bending and h) a sensor array attached on hand to detect touching location. Reproduced with permission.^[43] Copyright 2014, Wiley-VCH GmbH.

Stretchable resistance strain sensors for aquatic environments were developed based on conductive fluoropolymer gels. Cao et al. fabricated a sensing material, namely “GLASSES”, which is composed of fluorocarbon elastomer absorbed with fluorine-rich ionic liquids.^[79] It has the conductivity of $10^{-3} \text{ S cm}^{-1}$ and can be stretched to 2000%. It is fast self-healing in wet, acidic and alkali environments through the strong and reversible interaction between the dipoles of the polymer chains and ionic liquids. It was demonstrated to perform as touch, pressure and strain sensor in aquatic environment. Yu et al. fabricated ionogels through polymerization of fluorine-rich ionic liquid monomers in another fluorine-rich ionic liquids.^[86] The hydrophobic ionogels exhibit excellent properties, including adjustable mechanical properties, underwater self-healing, adhesiveness, transparency, and conductivity. The optical camouflage underwater resistance sensors were developed, and demonstrated to be used as human-machine interactive communicator in the aquatic environment.

Capacitive sensing technology is often used to prepare pressure or strain sensors with high sensitivity and high resolution, allowing long-term, and drift-free sensing when temperature changes.^[42,43] Sun et al. first reported a hydrogel capacitive sensor.^[43] It has a sandwich structure: a dielectric elastomer film (VHB 4905 3M) is stuck between two hydrogel layers (Figure 4e), which are polyacrylamide hydrogels containing NaCl. The voltage is applied on the sensor, and the capacitance (C) between two metal electrodes is measured. The working principle of the sensor is the relation between deformation and capacitance. Briefly, when it is stretched to λ times its initial length, both its thickness and width reduce by a factor of $\lambda^{1/2}$, so the capacitance scales as $C = C_0 \lambda$; when it is equi-biaxially stretched to λ times in both directions, the capacitance scales as $C = C_0 \lambda^4$ (Figure 4f); as it is compressed in thickness, its area expanded, and the

capacitance increased under pressure (Figure 4f). Because both materials are highly stretchable and compliant, the sensors are able to attach to fingers to detect the repeat bending (Figure 4g). The sensors were also fabricated into an array to demonstrate the capability of locating finger position (Figure 4h).

The capacitance sensor technology has been applied to a variety of conductive gel materials to develop a variety of sensors. Lei et al. synthesized supramolecular ionic conductive hydrogels by copolymerizing acrylic acid and zwitterionic monomer 3-dimethyl(methacryloyloxyethyl) ammonium propane sulfonate (DMAPS) in water and further immersing the obtained hydrogels in NaCl aqueous solutions until equilibration.^[87] The hydrogels have tunable mechanical properties, including robust elasticity, large stretchability, self-healability, flexible reconfiguration ability, and recyclability.^[87] The hydrogels were integrated into a sandwiched configuration, capable of sensing mechanical deformation both from parallel-plate capacitance and resistive signals changes. Furthermore, they chose ionic liquid as solvent for supramolecular networks, took advantage of the synergistic effect between conductive zwitterionic nanochannels and dynamic hydrogen-bonding networks, developed transparent (>90%, transmittance), and ultra-stretchable (>1000%, strain) conductor, and made a deformable sensory system by using the multi-layer capacity sensor design.^[88]

3.2. Temperature Sensors

Temperature perception is crucial for human-beings and animals to live in changed and complex bad weathers, similarly is crucial for soft robots. One of the most studied gel temperature sensors relies on the change of ionic conductivity induced by

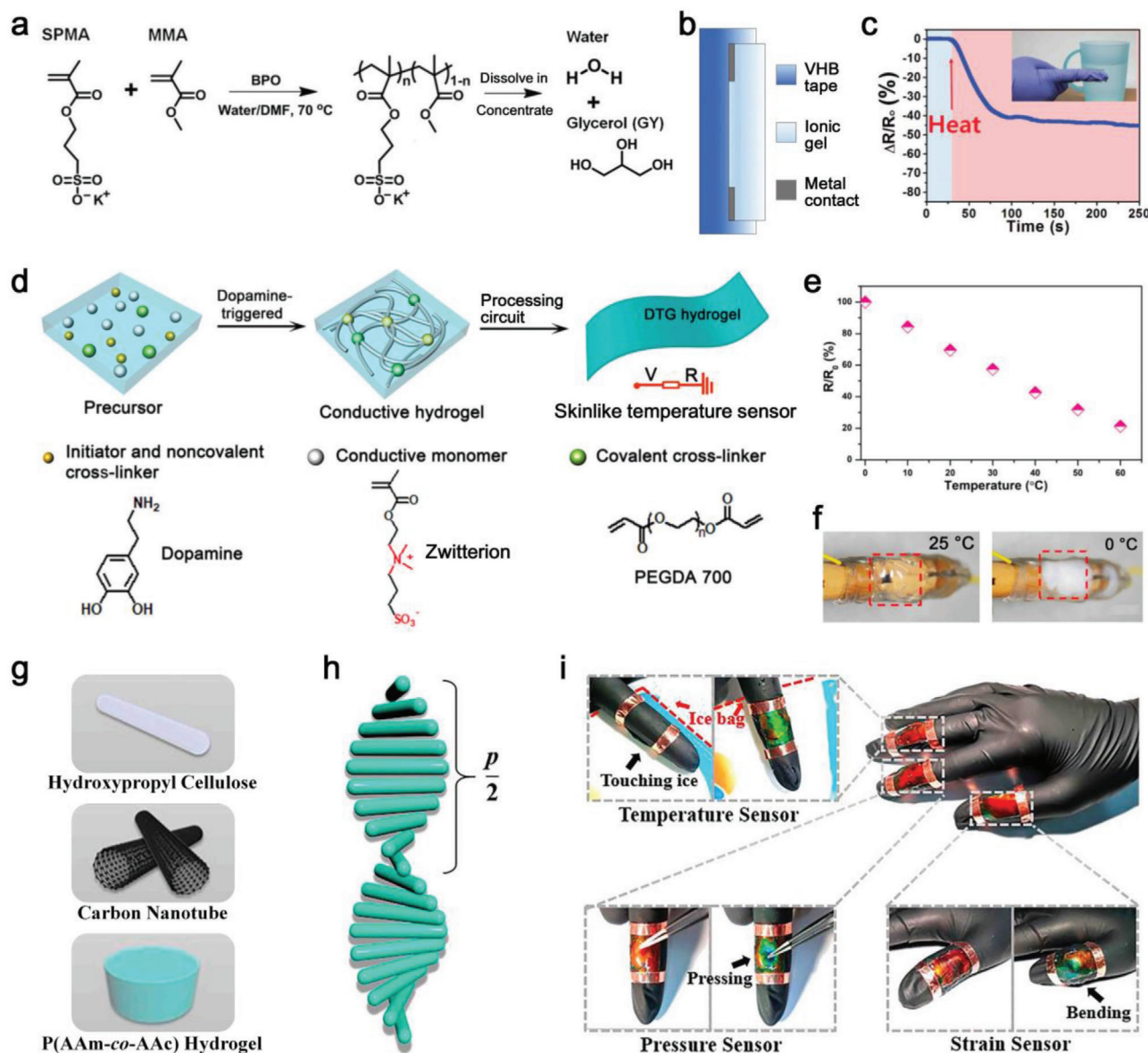


Figure 5. Schematics of a) synthesis of P(SPMA-*r*-MMA)s, preparing of corresponding gel, and b) temperature sensor.^[90] c) Response curve as the sensor touched to a hot cup. Reproduced with permission.^[90] Copyright 2019, Wiley-VCH GmbH. d) Schematic of preparing of dopamine-triggered polyzwitterion hydrogel and corresponding temperature sensor.^[45] e) Electrical resistance as a function of temperature.^[45] f) Photos of a sensor at 25 and 0 °C. Reproduced with permission.^[45] Copyright 2021, American Chemical Society. g) Schematic of composition of the structural color hydrogel, and h) the helical nanostructure of hydroxypropyl cellulose in hydrogel.^[91] i) Photos of the structural color hydrogels were used as temperature, pressure, and strain sensors. Reproduced with permission.^[91] Copyright 2020, National Academy of Sciences.

temperature.^[45,89] Lee et al. reported a polymer gel temperature sensor (Figure 5a,b), whose resistance increases with temperature increasing (Figure 5c), which phenomenon is resulted from the accelerated dynamic motion of the ions in gels.^[90] The polymers are made by copolymerizing 3-sulfopropyl methacrylate potassium salt (SPMA) and methyl methacrylate (MMA) (Figure 5a). The polymer matrix (P(SPMA-*r*-MMA)s) is physically cross-linked by ion cross-linking and entanglement, and absorbed with glycerol aqueous solution. The gel is transparent, stretchable, self-healing, and thermally stable. Glycerol with boiling point of 290 °C plays a role of plasticizer without evaporation.

Zhang et al. developed a dopamine-triggered polyzwitterion hydrogel (Figure 5d) and demonstrated its potential application as skin-like temperature sensor (Figure 5e,f).^[45] Therein, dopamine serves as a polymerization initiator by the virtue of free radicals generated from the self-oxidation process. The hydrogel is covalently cross-linked by poly(ethylene glycol) diacrylate (PEGDA), and noncovalently cross-linked by dopamine as it forms supramolecular interactions such as hydrogen bonding, cation- π interaction and aromatic interaction (Figure 5d). The electrical resistance of hydrogel is highly sensitive to vary temperature from 0 to 60 °C (Figure 5e). It suggests that temperature affects the

mobility of charged groups on polymers, and results in altering of ionic conductivity of hydrogel. Furthermore, the transparent hydrogel shows a transparent-opaque transition with upper critical solution temperature (UCST) of 7.8 °C (Figure 5f). Hence, the self-adhesion, self-healing and thermo-responsive hydrogel is expected to be used as visual skin-like sensors.

Standard fabrication of gel sensor with controllable thickness and high yield is a challenge due to the difficulty to machine the soft gels into precise samples. Wang et al. developed cryo-microtomy method to continuously make hydrogel sensors.^[67] Polyvinyl alcohol (PVA) / multi-walled carbon nanotube (MWCNT) composite hydrogel was prepared, and sectioned into pieces at -30 °C. The hydrogel is sensible to temperature variation, as temperature rising leads to accelerated carriers hopping and decreased resistance. The pieces showed controllable thicknesses from 0.5 to 600 μm, high yield of 20 pieces min⁻¹, and were used as temperature sensors to endow prosthesis to perceive and withdraw heat source.

Another type of impressive temperature sensor is designed based on the changes of cholesteric liquid-crystal nanostructure, which results in the change of structural color. Zhao et al. fabricated a structural color hydrogel that was constructed by incorporating hydroxypropyl cellulose (HPC), carbon nanotube (CNT) and poly(acrylamide-co-acrylic acid) hydrogel (Figure 5g).^[91] The HPC molecules form cholesteric liquid crystal phase, arranged in layers and periodically stacked into spiral structures in hydrogel (Figure 5h). The reflection wavelength of light, that is, the color of hydrogel is regulated by the helical pitch (P , Figure 5h) of cholesteric liquid crystal. It suggests that the rise of temperature breaks of hydrogen bonds between amide and carboxyl groups in hydrogel, expands in volume of hydrogel, increases in helical pitch of HPC, and finally results in the redshift of hydrogel color, whose process is reversible. A piece of hydrogel attached to finger was used to detect temperature, showed significant color change when contacted with an ice bag (Figure 5i). The hydrogel also responded to pressure and tension, as its deformation would lead to the change in internal nanostructure, and further result in color shift (Figure 5i).

3.3. Position Sensors

Mammals can sense the touch position precisely on their skins,^[1] which is very important for them to avoid obstacles and physical injuries. Position sensing technologies are common in touch pads and touch panels, which are requisite input devices for computers, mobile phones, smart appliances, point-of-information, and point-of-sale terminals. Indium tin oxide (ITO) has been mostly used as the transparent conductive film for manufacturing of commercial touch pads or panels based on projected capacitive touch (PCT) or surface capacitive touch (SCT) technologies. However, ITO is brittle, can't be bent or folded, and suffers from the risk of smash when dropped or be impacted. There is a great need to develop flexible position sensors for soft and wearable electronic intelligent devices.

PCT technology is widely used in touch panels of mobile phones and laptops, and is built on the concept of sensor arrays. The biggest merit of PCT technology is multi-touch, but it must be subjected to lithography and etching to produce patterns on

ITO. Sarwar et al. reported a flexible PCT sensor array, which composed of ionically conductive electrodes embedded in PDMS shells, with the column and row electrodes separated by a PDMS dielectric sheet (Figure 6a).^[17] The electrode is polyacrylamide hydrogels containing dissolved NaCl. The transparent sensor array reflects the touch and movement of fingers through the localized decrease in capacitances (Figure 6b), and the touch is detectable during bending and stretch. In the sensor array, each array element is composed of a disc-shaped electrode (Figure 6b, red) separated from a loop-shaped electrode (Figure 6b, blue) by a dielectric layer, producing a field that extends beyond the sensor surface. A finger acts as a third electrode that capacitively couples (capacitor C_F , Figure 6b) to the array element, reducing the coupling between electrodes (capacitor C_M , Figure 6b). The direction and magnitude of the capacitance change make it distinguishable from effects due to changes resulting from stretch or bend of the sensor. Furthermore, the sensor array exhibits multi-touch capability (Figure 6c) as is common in mobile phone touch screen.

However, present flexible sensor arrays suffer from the drawback of low resolution, thus are ill-suited for touch pads or touch panels. There are only 16 pixels in 4 cm square for the reported flexible PCT sensor arrays. Similar low resolution limitation also exists in other polymer-based touch pads, such as poly(vinylidene fluoride-co-trifluoroethylene) piezoelectric sensor (6 pixels in 10 × 7 cm² rectangle),^[93] elastomer capacitive sensor (9 pixels in 3 cm square),^[94] and cross-line array of fabric triboelectric generators (49 pixels in 10 cm square).^[95] In general, polymer materials are incompatible with standard photolithography microfabrication technology,^[33] making it highly challenging to produce high-density sensor arrays.^[96,97]

The input resolution of a touch pad based on SCT technology is not limited by the density of array points. Our group reported a SCT hydrogel touch pad.^[92] A 1D sensor in Figure 6d demonstrates the architecture structure and working principle of the SCT sensor. Each end of a hydrogel strip is connected to an external resistance (R_e) through a metal electrode, then, both sides are connected to the same AC power (Figure 6d). The same phase and high frequency AC voltage (± 0.6 V, 17 kHz) generated from the power is applied on the circuit. When a finger touches the conductive hydrogel, there is a coupling capacitor (C_{finger}) in the interface of finger and hydrogel, and the circuit is grounded through the finger. The conductive hydrogel is essentially a resistance (R_{gel}), divided by the finger into left and right parts. The resistance of each part is proportional to its normalized length (x , $1-x$) (Figure 6d). The left and right hydrogel parts are connected in parallel, and respectively connected to a R_e in series. The voltages on two parallel circuits are equal, as a result, when the finger moves to right, xR_{gel} increases (Figure 6d), and the voltage on the left R_e decreases (Figure 6e), correspondingly, $(1-x)R_{gel}$ decreases, and the voltage on the right R_e increases. Therefore, the x value, that is, the finger position could be determined from the voltage measured on R_e . PDMS film was covered on hydrogel surface to provide comfortable touch feeling. In the presence of PDMS, there is still a C_{finger} between finger and hydrogel, and the system still has position sensing capability.

The conductive hydrogel for SCT touch pad is prepared by polymerizing zwitterion monomers in aqueous solution of nano-clays. The polyzwitterion-clay nanocomposite hydrogel

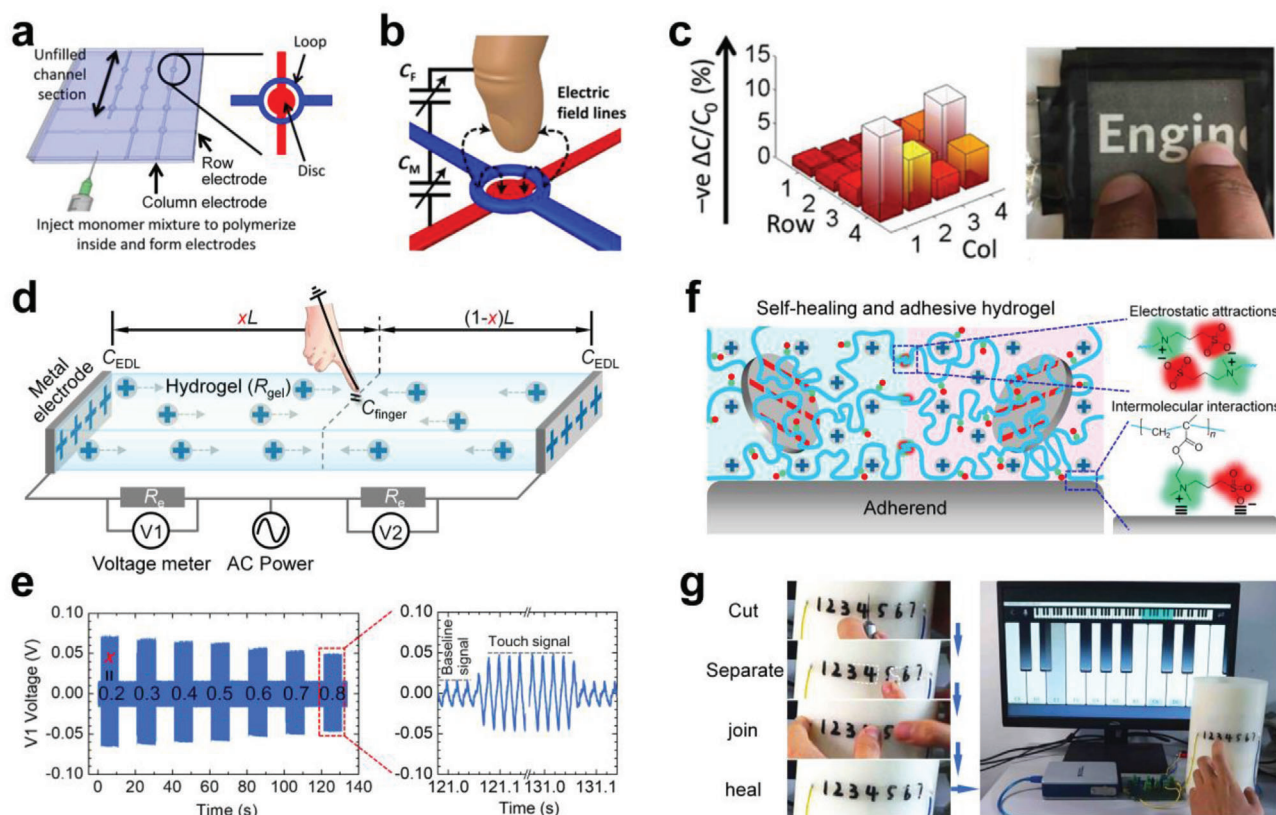


Figure 6. Schematic illustration of a) fabrication and b) sensing mechanism of PCT sensor array.^[17] Finger approaching an array point leads to reducing of coupling capacitance (C_M) between the upper and under hydrogel electrodes. c) The change of capacitance as two fingers touch the sensor simultaneously, demonstrating multi-touch capability. Reproduced with permission.^[17] Copyright 2017, AAAS. d) The architecture of a 1D SCT hydrogel position sensor, and e) corresponding V1 voltage changed by finger touch position.^[92] f) Schematic illustration of the structure, self-healing and adhesive mechanism of polyzwitterion-clay nanocomposite hydrogel.^[92] g) Photos show a hydrogel strip adhered on a plastic rod was cut then joined, and used to play a piano game. Reproduced with permission.^[92] Copyright 2020, Wiley-VCH.

is reversibly cross-linked by the reversible physical adsorption between polymers and exfoliated nano-clays. It could be stretched to strain beyond 1500%, and is self-healable through reconstruction of supramolecular crosslinking at cut-then-joined interfaces (Figure 6f). It is also adhesive to various solid surfaces, because the long polymer chains in viscoelastic matrixes provide intermolecular interaction mechanisms based on van der Waals' force, electrostatic force and hydrogen bonding (Figure 6f). It has a high transparency (98.8%) for the uniform nano-clays which are dissolved other than aggregated in matrixes. The Na^+ originated from nano-clays act as ionic carriers and provide a conductivity of 0.14 S m^{-1} . A self-healed hydrogel strip adhered on a nylon rod was demonstrated to be used to play piano game by taking advantage of the position sensing function (Figure 6g). 2D hydrogel position sensor was also prepared by simultaneously locating a finger in transverse and longitudinal directions.

Kim et al. demonstrated that the SCT technology could still works when the conductive hydrogel is stretched to >1000% areal strain.^[16] Cao et al. fabricated touch panel that works in aquatic environment by the same SCT position sensor technology.^[79] The Jiang group developed a flexible SCT touch panel by using vermiculite nano-clay membrane as the transparent conductive material.^[98]

3.4. Multifunctional Sensing Devices

Somatosensory system of human skin can distinguish various stimuli such as pressure, stretch, pinch, force, temperature, humidity, etc.,^[1,3] because there are a large number of receptors with different functions spatially distributed in the dermis. Electronic skin that fully imitates human somatosensory functions is highly desired for haptic devices, wearable health care sensors, prostheses, and neuromuscular systems in soft robotics. At present, multimodal bionic skin sensors have obtained progress in two design strategies. One is integrating different types of sensors,^[85,99] another is decoupling independent variables for differentiating various sensing information simultaneously from a single sensor unit.^[100]

Lei et al. developed a type of polyionic elastomers with multiple sensations.^[101] The polyionic elastomer was prepared by polymerization of cationic monomers methyl chloride quaternized *N,N*-dimethylamino ethylacrylate (DMAEA-Q) in aqueous solution of anionic polyacrylic acid, followed by drying in ambient conditions for determined times. The synthesized viscous liquid was used as precursor ink for 3D printing. Polyionic sensors that mimic mechanoreceptors, humidity receptor and thermo-receptor of human skin were prepared by 3D printing

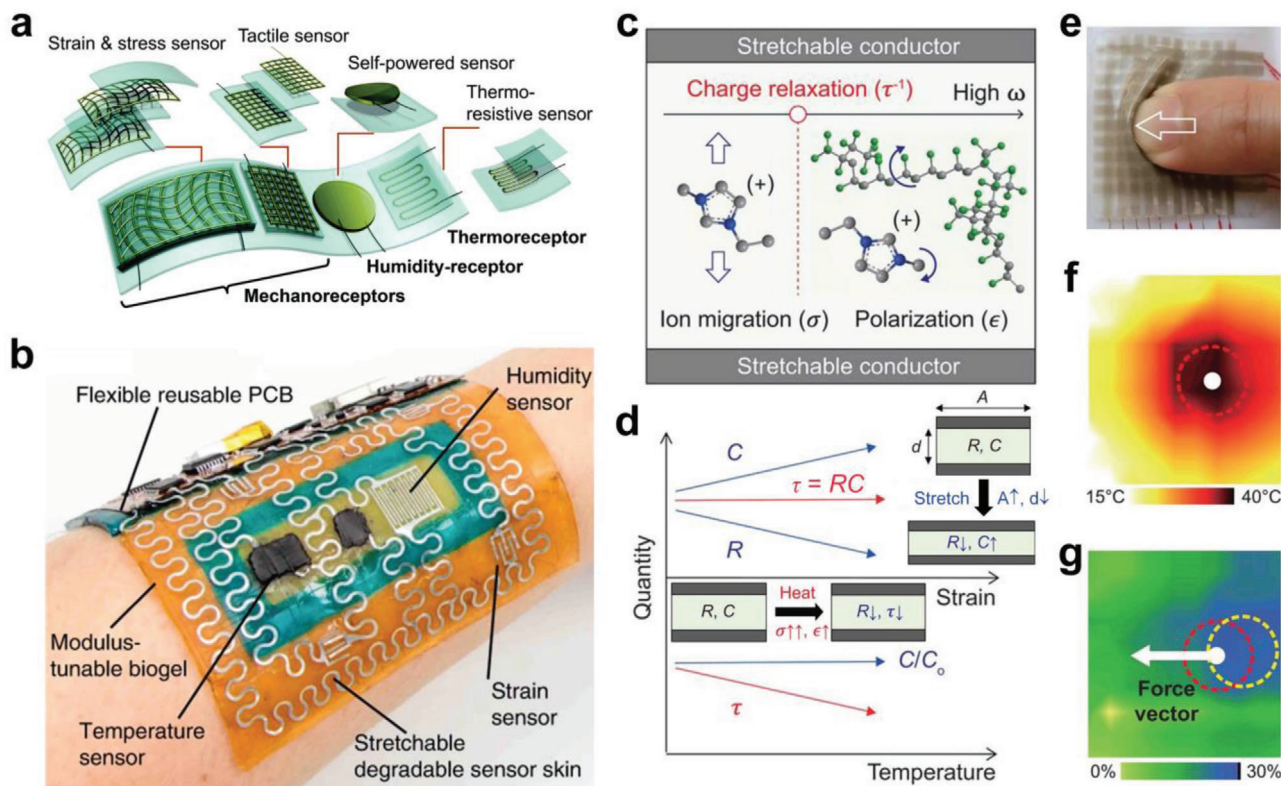


Figure 7. a) Schematic design of the multiple flexible sensation combining different bionic receptors. Green layers and golden parts represent VHB tapes and 3D-printing polyionic elastomers, respectively. Reproduced with permission.^[101] Copyright 2019, The Royal Society of Chemistry. b) A photo of multimodal e-skin integrating of temperature, humidity, and strain sensors on gelatin-based biogel. Reproduced with permission.^[85] 2020, Nature Publishing Group. c) A schematic of multimodal ionic receptor. d) Schemes and conceptual plots of the strain-insensitive variable (τ , top) and the temperature-insensitive variable (C/C_0 , bottom) of the ionic receptor. e) Photo, f) 2D temperature profile, and g) 2D strain profile of a multimodal receptor array under a unidirectional shear applied with a forefinger. Reproduced with permission.^[100] Copyright 2020, American Association for the Advancement of Science.

and integrated in a dielectric film (Figure 7a). The polyionic skin show multiple sensations towards strain, pressure, touch, humidity, and temperature.^[101] The humidity sensor works based on a principle of self-powered phenomenon: moisture promotes the ionization of one side of the polyionic elastomer, in which more free ions are released, the migration of ions to another side induces voltage creation.

Baumgartner et al. developed a highly resilient gelatin-based biogel, and manufactured a biodegradable, stretchable multimodal e-skin, which had temperature, humidity and strain sensors by using the biogel (Figure 7b).^[85] The biogel was prepared by mixing gelatin powder with a presolution consisting of citric acid, sugar syrup, glycerol, and water, followed by drying on Teflon plate to obtain a film. The sensors, structured from patterning zinc foil or temperature-sensitive paste, were integrated on a biogel patch (Figure 7b). The multimodal e-skin may provide information about temperature, humidity or the state of deformation to robots. Tseng et al. fabricated a series of sensors with pressure, sweat and temperature perceptions.^[102] By embedding those sensors within additional hydrogel layers, they realized multifunctional e-skin in one system.

You et al. presented an artificial multimodal ionic receptor that can differentiate thermal and mechanical change without signal interference.^[100] The multimodal receptor was composed of an

ion conductor layer (e-PVDF-HFP containing ionic liquid) that sandwiched between two stretchable electrodes (Ag nanowires / SEBS composites) (Figure 7c), and was fabricated by multi-step spin coating. The charge relaxation time ($\tau = \epsilon/\sigma$, ϵ is dielectric constant, σ is ion conductivity) is a strain-insensitive variable for detecting temperature (Figure 7d). The normalized capacitance (C/C_0 , $C = \epsilon A/d$, A is area, d is thickness) is a temperature-insensitive variable for sensing the strain (Figure 7d). τ and C/C_0 allow simultaneous monitoring of mechanical and thermal changes. A 10-by-10 multimodal receptor array was demonstrated to be used to recognize the pinch gesture. For example, a directional shear was applied with a forefinger on the array (Figure 7e). The contact point was identified as the highest-temperature point in temperature profile (Figure 7f,g). From the strain profile, the stretched region is located behind the contact point (Figure 7h). Therefore, unidirectional shear induced by the finger could be recognized. Other tactile motions such as shear, spread and torsion were also recognized on the array surface by the similar method.

4. Summary and Outlook

We have outlined the main strategies to prepare conductive polymer gels and corresponding flexible single and multifunctional

sensors, and highlighted the important recent progress in the field. Researchers have developed a series of conductive polymer gels with tunable electronic and mechanical properties, and a wide variety of pressure and strain sensors, temperature sensors, position sensors and multifunctional sensors that more closely mimic the functions and capabilities of human skin. Though not introduced in detail here, significant progress has also been made in many other interesting bionic skin sensors based on polymer gels, such as humidity sensors^[51,52] and taste sensors.^[103]

While a great deal has already been achieved, there are remaining challenges to be explored. First, it is a challenge to fully mimic skin performance. For example, present gel sensors can not make oxygen permeate and sweat out like skin; no polymer gels-based sensors fully achieve non-toxic, low- and high- temperature resistance, and work in aquatic environment. Solving these problems depends on the systematic analysis, study and imitation of the molecular and microscopic structures of the skin. Secondly, multimodal sensing is an important direction to work on. When an object touches our skin, we immediately feel the temperature, humidity, shape, surface texture, touch position, and touch force of the object through the skin sensing system. The reported multifunction sensors mainly rely on integration of different sensors in plane direction, and they cannot perceive multiple information at one touch point. One approach to address this challenge is to develop multi level array sensor assembly. To realize this, advanced manufacturing techniques beyond 3D printing^[1,104,105] and ink-jet printing^[42,106] are in urgent demand. The third major challenge is closed loop control. We use brain to interpret sensing signals, and use it as basis for directing the muscle to produce meaningful actions. The use of flexible sensors for closed-loop control is still in its infancy.

We believe that in the near future, flexible sensors will be widely worn in human body. These smart devices will expand the way we perceive and interact with the world in the same way that our eyes, ears, nose, tongue, and skin once did.

Acknowledgements

This work was supported financially by National Natural Science Foundation of China (51773215), Key Research Program of Frontier Sciences, Chinese Academy of Sciences (QYZDB-SSW-SLH036), Zhejiang Provincial Natural Science Foundation of China (LY21E030013), Ningbo Scientific and Technological Innovation 2025 Major Project (2020Z022), Ningbo Natural Science Foundation (202003N4359), the Sino-German Mobility Program (M-0424), and K.C.Wong Education Foundation (GJTD-2019-13).

Conflict of Interest

The authors declare no conflict of interest.

Keywords

bionic skins, conductive polymers, gels, ionic conductors, sensors

Received: July 23, 2021

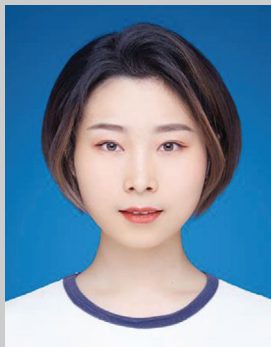
Revised: August 30, 2021

Published online: September 20, 2021

- [1] A. Zimmerman, L. Bai, D. D. Ginty, *Science* **2014**, *346*, 950.
- [2] R. S. Dahiyia, G. Metta, M. Valle, G. Sandini, *IEEE Trans. Robot.* **2010**, *26*, 1.
- [3] A. Chortos, J. Liu, Z. Bao, *Nat. Mater.* **2016**, *15*, 937.
- [4] M. L. Hammock, A. Chortos, B. C. Tee, J. B. Tok, Z. Bao, *Adv. Mater.* **2013**, *25*, 5997.
- [5] X. Liu, *Science* **2020**, *370*, 910.
- [6] J. X. Wang, M. F. Lin, S. Park, P. S. Lee, *Mater. Today* **2018**, *21*, 508.
- [7] X. Le, W. Lu, J. Zhang, T. Chen, *Adv. Sci.* **2019**, *6*, 1801584.
- [8] S. Yao, P. Ren, R. Song, Y. Liu, Q. Huang, J. Dong, B. T. O'Connor, Y. Zhu, *Adv. Mater.* **2020**, *32*, 1902343.
- [9] R. Yin, D. Wang, S. Zhao, Z. Lou, G. Shen, *Adv. Funct. Mater.* **2020**, *31*, 2008936.
- [10] J. Wang, C. Yan, G. Cai, M. Cui, A. Lee-Sie Eh, P. S. Lee, *Adv. Mater.* **2016**, *28*, 4490.
- [11] Y. Gao, L. Shi, S. Lu, T. Zhu, X. Da, Y. Li, H. Bu, G. Gao, S. Ding, *Chem. Mater.* **2019**, *31*, 3257.
- [12] Y. Ren, J. Guo, Z. Liu, Z. Sun, Y. Wu, L. Liu, F. Yan, *Sci. Adv.* **2019**, *5*, 0648.
- [13] C. Keplinger, J.-Y. Sun, C. C. Foo, P. Rothmund, G. M. Whitesides, Z. Suo, *Science* **2013**, *341*, 984.
- [14] T. Li, Y. Wang, S. Li, X. Liu, J. Sun, *Adv. Mater.* **2020**, *32*, 2002706.
- [15] H. Yuk, B. Lu, X. Zhao, *Chem. Soc. Rev.* **2019**, *48*, 1642.
- [16] C. C. Kim, H. H. Lee, K. H. Oh, J. Y. Sun, *Science* **2016**, *353*, 682.
- [17] M. S. Sarwar, Y. Dobashi, C. Preston, J. K. M. Wyss, S. Mirabbasi, J. D. W. Madden, *Sci. Adv.* **2017**, *3*, e1602200.
- [18] N. Holten-Andersen, M. J. Harrington, H. Birkedal, B. P. Lee, P. B. Messersmith, K. Y. Lee, J. H. Waite, *Proc. Natl. Acad. Sci. U. S. A.* **2011**, *108*, 2651.
- [19] J. Y. Sun, X. Zhao, W. R. Illeperuma, O. Chaudhuri, K. H. Oh, D. J. Mooney, J. J. Vlassak, Z. Suo, *Nature* **2012**, *489*, 133.
- [20] J. R. McKee, E. A. Appel, J. Seitsonen, E. Kontturi, O. A. Scherman, O. Ikkala, *Adv. Funct. Mater.* **2014**, *24*, 2706.
- [21] L. Voorhaar, R. Hoogenboom, *Chem. Soc. Rev.* **2016**, *45*, 4013.
- [22] Y. Wang, S. Lee, T. Yokota, H. Wang, Z. Jiang, J. Wang, M. Koizumi, T. Someya, *Sci. Adv.* **2020**, *6*, 7043.
- [23] G. Ge, Y. Z. Zhang, W. Zhang, W. Yuan, J. K. El-Demellawi, P. Zhang, E. Di Fabrizio, X. Dong, H. N. Alshareef, *ACS Nano* **2021**, *15*, 2698.
- [24] Y. Jian, B. Wu, X. Le, Y. Liang, Y. Zhang, D. Zhang, L. Zhang, W. Lu, J. Zhang, T. Chen, *Research* **2019**, *2019*, 2384347.
- [25] H. Wei, M. Lei, P. Zhang, J. Leng, Z. Zheng, Y. Yu, *Nat. Commun.* **2021**, *12*, 2082.
- [26] J. Wen, J. Tang, H. Ning, N. Hu, Y. Zhu, Y. Gong, C. Xu, Q. Zhao, X. Jiang, X. Hu, L. Lei, D. Wu, T. Huang, *Adv. Funct. Mater.* **2021**, *31*, 2011176.
- [27] Y. Ye, Y. Zhang, Y. Chen, X. Han, F. Jiang, *Adv. Funct. Mater.* **2020**, *30*, 2003430.
- [28] Y. Cao, T. G. Morrissey, E. Acome, S. I. Allec, B. M. Wong, C. Keplinger, C. Wang, *Adv. Mater.* **2017**, *29*, 1605099.
- [29] K. H. Lee, Y. Z. Zhang, Q. Jiang, H. Kim, A. A. Alkenawi, H. N. Alshareef, *ACS Nano* **2020**, *14*, 3199.
- [30] T. Sekitani, T. Yokota, K. Kuribara, M. Kaltenbrunner, T. Fukushima, Y. Inoue, M. Sekino, T. Isoyama, Y. Abe, H. Onodera, T. Someya, *Nat. Commun.* **2016**, *7*, 11425.
- [31] B. Lu, H. Yuk, S. Lin, N. Jian, K. Qu, J. Xu, X. Zhao, *Nat. Commun.* **2019**, *10*, 1043.
- [32] B. C. Tee, C. Wang, R. Allen, Z. Bao, *Nat. Nanotechnol.* **2012**, *7*, 825.
- [33] V. R. Feig, H. Tran, M. Lee, Z. Bao, *Nat. Commun.* **2018**, *9*, 2740.
- [34] Y. Liu, J. Liu, S. Chen, T. Lei, Y. Kim, S. Niu, H. Wang, X. Wang, A. M. Foudeh, J. B. Tok, Z. Bao, *Nat. Biomed. Eng.* **2019**, *3*, 58.
- [35] L. Pan, A. Chortos, G. Yu, Y. Wang, S. Isaacson, R. Allen, Y. Shi, R. Dauskardt, Z. Bao, *Nat. Commun.* **2014**, *5*, 3002.

- [36] D. Mawad, C. Mansfield, A. Lauto, F. Perbellini, G. W. Nelson, J. Tonkin, S. O. Bello, D. J. Carrad, A. P. Micolich, M. M. Mahat, J. Furman, D. J. Payne, A. R. Lyon, J. J. Gooding, S. E. Harding, C. M. Terracciano, M. M. Stevens, *Sci. Adv.* **2016**, *2*, e1601007.
- [37] H. Qin, T. Zhang, N. Li, H. P. Cong, S. H. Yu, *Nat. Commun.* **2019**, *10*, 2202.
- [38] T. B. H. Schroeder, A. Guha, A. Lamoureux, G. VanRenterghem, D. Sept, M. Shtein, J. Yang, M. Mayer, *Nature* **2017**, *552*, 214.
- [39] Z. Lei, W. Zhu, X. Zhang, X. Wang, P. Wu, *Adv. Funct. Mater.* **2020**, *31*, 2008020.
- [40] H. J. Kim, B. Chen, Z. Suo, R. C. Hayward, *Science* **2020**, *367*, 773.
- [41] J. Duan, W. Xie, P. Yang, J. Li, G. Xue, Q. Chen, B. Yu, R. Liu, J. Zhou, *Nano Energy* **2018**, *48*, 569.
- [42] C. Larson, B. Peele, S. Li, S. Robinson, M. Totaro, L. Beccai, B. Maz-zolai, R. Shepherd, *Science* **2016**, *351*, 1071.
- [43] J. Y. Sun, C. Keplinger, G. M. Whitesides, Z. Suo, *Adv. Mater.* **2014**, *26*, 7608.
- [44] X. Pu, M. Liu, X. Chen, J. Sun, C. Du, Y. Zhang, J. Zhai, W. Hu, Z. L. Wang, *Sci. Adv.* **2017**, *3*, e1700015.
- [45] C. Zhang, Y. Zhou, H. Han, H. Zheng, W. Xu, Z. Wang, *ACS Nano* **2021**, *15*, 1785.
- [46] G. Ge, Y. Zhang, J. Shao, W. Wang, W. Si, W. Huang, X. Dong, *Adv. Funct. Mater.* **2018**, *28*, 1802576.
- [47] Z. Zhang, L. Wang, H. Yu, F. Zhang, L. Tang, Y. Feng, W. Feng, *ACS Appl. Mater. Interfaces* **2020**, *12*, 15657.
- [48] Q. Zhang, X. Liu, L. Duan, G. Gao, *J. Mater. Chem. A* **2020**, *8*, 4515.
- [49] Y. Liang, L. Ye, X. Sun, Q. Lv, H. Liang, *ACS Appl. Mater. Interfaces* **2020**, *12*, 1577.
- [50] N. T. Nguyen, M. S. Sarwar, C. Preston, A. Le Goff, C. Plesse, F. Vidal, E. Cattani, J. D. W. Madden, *Extreme Mech. Lett.* **2019**, *33*, 100574.
- [51] M. J. Yin, Z. R. Li, T. R. Lv, K. T. Yong, Q. F. An, *Sens. Actuators, B* **2021**, *339*, 129887.
- [52] M. Ju, B. H. Wu, S. T. Sun, P. Y. Wu, *Adv. Funct. Mater.* **2020**, *30*, 1910387.
- [53] Y. J. Peng, M. H. Pi, X. L. Zhang, B. Yan, Y. S. Li, L. Y. Shi, R. Ran, *Polymer* **2020**, *196*, 122469.
- [54] Z. Lei, Q. Wang, S. Sun, W. Zhu, P. Wu, *Adv. Mater.* **2017**, *29*, 1700321.
- [55] Y. Z. Zhang, K. H. Lee, D. H. Anjum, R. Sougrat, Q. Jiang, H. Kim, H. N. Alshareef, *Sci. Adv.* **2018**, *4*, eaat0098.
- [56] H. Lu, B. Wu, X. Yang, J. Zhang, Y. Jian, H. Yan, D. Zhang, Q. Xue, T. Chen, *Small* **2020**, *16*, e2005461.
- [57] V. Amoli, J. S. Kim, E. Jee, Y. S. Chung, S. Y. Kim, J. Koo, H. Choi, Y. Kim, D. H. Kim, *Nat. Commun.* **2019**, *10*, 4019.
- [58] K. Parida, V. Kumar, W. Jiangxin, V. Bhavanasi, R. Bendi, P. S. Lee, *Adv. Mater.* **2017**, *29*, 1702181.
- [59] Q. Wang, X. Pan, H. Zhang, S. Cao, X. Ma, L. Huang, L. Chen, Y. Ni, *J. Mater. Chem. A* **2021**, *9*, 3968.
- [60] X. Y. Yin, Y. Zhang, J. Xiao, C. Moorlag, J. Yang, *Adv. Funct. Mater.* **2019**, *29*, 1904716.
- [61] W. Zhang, B. Wu, S. Sun, P. Wu, *Nat. Commun.* **2021**, *12*, 4082.
- [62] Y. Ren, Z. Liu, G. Jin, M. Yang, Y. Shao, W. Li, Y. Wu, L. Liu, F. Yan, *Adv. Mater.* **2021**, *33*, 2008486.
- [63] B. Yiming, Y. Han, Z. Han, X. Zhang, Y. Li, W. Lian, M. Zhang, J. Yin, T. Sun, Z. Wu, T. Li, J. Fu, Z. Jia, S. Qu, *Adv. Mater.* **2021**, *33*, 2006111.
- [64] G. Gu, N. Zhang, H. Xu, S. Lin, Y. Yu, G. Chai, L. Ge, Y. H. Q. Shao, X. Sheng, X. Zhu, X. Zhao, *Nat. Biomed. Eng.* **2021**, <https://doi.org/10.1038/s41551-021-00767-0>.
- [65] T. Li, G. Li, Y. Liang, T. Cheng, J. Dai, X. Yang, B. Liu, Z. Zeng, Z. Huang, Y. Luo, T. Xie, W. Yang, *Sci. Adv.* **2017**, *3*, e1602045.
- [66] Y. Ohm, C. Pan, M. J. Ford, X. Huang, J. Liao, C. Majidi, *Nat. Electron.* **2021**, *4*, 185.
- [67] Y. Cai, J. Shen, C. W. Yang, Y. Wan, H. L. Tang, A. A. Aljarb, C. Chen, J. H. Fu, X. Wei, K. W. Huang, Y. Han, S. J. Jonas, X. Dong, V. Tung, *Sci. Adv.* **2020**, *6*, eabb5367.
- [68] H. Li, Y. Liang, G. Gao, S. Wei, Y. Jian, X. Le, W. Lu, Q. Liu, J. Zhang, T. Chen, *Chem. Eng. J.* **2021**, *415*, 128988.
- [69] Y. Ma, Y. Gao, L. Liu, X. Ren, G. Gao, *Chem. Mater.* **2020**, *32*, 8938.
- [70] V. Guarino, M. A. Alvarez-Perez, A. Borriello, T. Napolitano, L. Ambrosio, *Adv. Healthcare Mater.* **2013**, *2*, 218.
- [71] C. Marin, E. Fernandez, *Front. Neuroeng.* **2010**, *3*, 8.
- [72] E. Castagnola, A. Ansaldo, E. Maggiolini, T. Ius, M. Skrap, D. Ricci, L. Fadiga, *Front. Neuroeng.* **2014**, *7*, 8.
- [73] S. C. Luo, E. M. Ali, N. C. Tansil, H. Yu, S. Gao, E. A. B. Kantchev, J. Y. Ying, *Langmuir* **2008**, *24*, 8071.
- [74] F. Greco, A. Zucca, S. Taccola, A. Menciassi, T. Fujie, H. Haniuda, S. Takeoka, P. Dario, V. Mattoli, *Soft Matter* **2011**, *7*, 10642.
- [75] D. Mawad, A. Artzy-Schnirman, J. Tonkin, J. Ramos, S. Inal, M. M. Mahat, N. Darwish, L. Zwi-Dantsis, G. G. Malliaras, J. J. Gooding, A. Lauto, M. M. Stevens, *Chem. Mater.* **2016**, *28*, 6080.
- [76] Q. Wu, J. Wei, B. Xu, X. Liu, H. Wang, W. Wang, Q. Wang, W. Liu, *Sci. Rep.* **2017**, *7*, 41566.
- [77] M. A. Leaf, M. Muthukumar, *Macromolecules* **2016**, *49*, 4286.
- [78] Y. Y. Lee, H. Y. Kang, S. H. Gwon, G. M. Choi, S. M. Lim, J. Y. Sun, Y. C. Joo, *Adv. Mater.* **2016**, *28*, 1636.
- [79] Y. Cao, Y. J. Tan, S. Li, W. W. Lee, H. Guo, Y. Cai, C. Wang, B. C. K. Tee, *Nat. Electron.* **2019**, *2*, 75.
- [80] M. Wang, Y. Luo, T. Wang, C. Wan, L. Pan, S. Pan, K. He, A. Neo, X. Chen, *Adv. Mater.* **2021**, *33*, 2003014.
- [81] H. Wei, Z. Wang, H. Zhang, Y. Huang, Z. Wang, Y. Zhou, B. B. Xu, S. Halila, J. Chen, *Chem. Mater.* **2021**, *33*, 6731.
- [82] Z. Wang, H. Cui, S. Li, X. Feng, J. Aghassi-Hagmann, S. Azizian, P. A. Levkin, *ACS Appl. Mater. Interfaces* **2021**, *13*, 21661.
- [83] Z. Wang, J. Chen, Y. Cong, H. Zhang, T. Xu, L. Nie, J. Fu, *Chem. Mater.* **2018**, *30*, 8062.
- [84] Z. Wang, J. Chen, L. Wang, G. Gao, Y. Zhou, R. Wang, T. Xu, J. Yin, J. Fu, *J. Mater. Chem. B* **2019**, *7*, 24.
- [85] M. Baumgartner, F. Hartmann, M. Drack, D. Preninger, D. Wirthl, R. Gerstmayr, L. Lehner, G. Mao, R. Pruckner, S. Demchyshyn, L. Reiter, M. Strobel, T. Stockinger, D. Schiller, S. Kimeswenger, F. Greibich, G. Buchberger, E. Bradt, S. Hild, S. Bauer, M. Kaltenbrunner, *Nat. Mater.* **2020**, *19*, 1102.
- [86] Z. Yu, P. Wu, *Adv. Mater.* **2021**, *33*, 2008479.
- [87] Z. Lei, P. Wu, *Nat. Commun.* **2018**, *9*, 1134.
- [88] Z. Lei, P. Wu, *Nat. Commun.* **2019**, *10*, 3429.
- [89] Y. Tan, Y. Zhang, Y. Zhang, J. Zheng, H. Wu, Y. Chen, S. Xu, J. Yang, C. Liu, Y. Zhang, *Chem. Mater.* **2020**, *32*, 7670.
- [90] J. Lee, M. W. M. Tan, K. Parida, G. Thangavel, S. A. Park, T. Park, P. S. Lee, *Adv. Mater.* **2020**, *32*, 1906679.
- [91] Z. Zhang, Z. Chen, Y. Wang, Y. Zhao, *Proc. Natl. Acad. Sci. U. S. A.* **2020**, *117*, 18310.
- [92] G. Gao, F. Yang, F. Zhou, J. He, W. Lu, P. Xiao, H. Yan, C. Pan, T. Chen, Z. L. Wang, *Adv. Mater.* **2020**, *32*, 2004290.
- [93] S. Gonçalves, J. Serrado-Nunes, J. Oliveira, N. Pereira, L. Hilliou, C. M. Costa, S. Lanceros-Méndez, *ACS Appl. Electron. Mater.* **2019**, *1*, 1678.
- [94] X. Wang, Y. Zhang, X. Zhang, Z. Huo, X. Li, M. Que, Z. Peng, H. Wang, C. Pan, *Adv. Mater.* **2018**, *30*, 1706738.
- [95] S.-B. Jeon, W.-G. Kim, S.-J. Park, I.-W. Tcho, I.-K. Jin, J.-K. Han, D. Kim, Y.-K. Choi, *Nano Energy* **2019**, *65*, 103994.
- [96] C. Pan, L. Dong, G. Zhu, S. Niu, R. Yu, Q. Yang, Y. Liu, Z. L. Wang, *Nat. Photonics* **2013**, *7*, 752.
- [97] Y.-Q. Zheng, Y. Liu, D. Zhong, S. Nikzad, S. Liu, D. L. Z. Yu, H.-C. Wu, C. Zhu, J. Li, H. Tran, J. B.-H. Tok, Z. Bao, *Science* **2021**, *373*, 88.
- [98] L. Cao, H. Wu, X. He, H. Geng, R. Zhang, M. Qiu, P. Yang, B. Shi, N. A. Khan, Z. Jiang, *J. Mater. Chem. A* **2019**, *7*, 25657.

- [99] Q. Hua, J. Sun, H. Liu, R. Bao, R. Yu, J. Zhai, C. Pan, Z. L. Wang, *Nat. Commun.* **2018**, *9*, 244.
- [100] M. I. You, D. G. Mackanic, N. Matsuhisa, J. Kang, J. Kwon, L. Beker, J. Mun, W. Suh, T. Y. Kim, J. B.-H. Tok, Z. Bao, U. Jeong, *Science* **2020**, *370*, 961.
- [101] Z. Lei, P. Wu, *Mater. Horiz.* **2019**, *6*, 538.
- [102] M. Dautta, M. Alshetaiwi, A. Escobar, F. Torres, N. Bernardo, P. Tseng, *Adv. Electron. Mater.* **2020**, *6*, 1901311.
- [103] J. Yeom, A. Choe, S. Lim, Y. Lee, S. Na, H. Ko, *Sci. Adv.* **2020**, *6*, eaba5785.
- [104] J. Odent, T. J. Wallin, W. Pan, K. Kruemplestaedter, R. F. Shepherd, E. P. Giannelis, *Adv. Funct. Mater.* **2017**, *27*, 1701807.
- [105] K. Tian, J. Bae, S. E. Bakarich, C. Yang, R. D. Gately, G. M. Spinks, M. In, H. Panhuis, Z. Suo, J. J. Vlassak, *Adv. Mater.* **2017**, *29*, 1604827.
- [106] T. Sekitani, H. Nakajima, H. Maeda, T. Fukushima, T. Aida, K. Hata, T. Someya, *Nat. Mater.* **2009**, *8*, 494.



Huijing Li received her B.S. degree from South China University of Technology University in 2018. Currently, she is a PhD student in the Ningbo Institute of Materials Technology and Engineering, Chinese Academy of Sciences, under the supervision Professor Tao Chen. Her current research interests focus on preparation of polymer-based hybrid materials and their applications in sensing and actuating.



Dr. Guorong Gao received his Ph.D. in polymer chemistry and physics from Ningbo Institute of Materials Technology and Engineering (NIMTE), Chinese Academy of Sciences in 2015. After that, he joined NIMTE as a postdoctoral research fellow. He was promoted to Associate professor in 2017. His current research is focused on the fabrication of high performance polymer ionic conductors for wearable electronic devices.



Prof. Tao Chen received his Ph.D. in polymer chemistry and physics from Zhejiang University in 2006. After his postdoctoral training at the University of Warwick (UK), he joined Duke University (USA) as a research scientist. He then moved back to Europe as an Alexander von Humboldt Research Fellow at Technische Universität Dresden, Germany. Since 2012, he is a full-time professor at Ningbo Institute of Materials Technology and Engineering, Chinese Academy of Sciences. His research interests include smart polymers and their hybrid systems with applications as actuators, shape memory polymers, and chemical sensing.